The Plant Cell, Vol. 13, 943–952, April 2001, www.plantcell.org © 2001 American Society of Plant Physiologists

The Pore of Plant K^+ Channels Is Involved in Voltage and pH Sensing: Domain-Swapping between Different K^+ Channel α-Subunits

Stefan Hoth,[1,2] Dietmar Geiger,[1] Dirk Becker, and Rainer Hedrich[3]

Molekulare Pflanzenphysiologie und Biophysik, Julius-von-Sachs-Institut für Biowissenschaften, Universität Würzburg, Julius-von-Sachs-Platz 2, D-97082 Würzburg, Germany

Plant K^+ uptake channel types differ with respect to their voltage, Ca^{2+}, and pH dependence. Here, we constructed recombinant chimeric channels between KST1, a member of the inward-rectifying, acid-activated KAT1 family, and AKT3, a member of the weakly voltage-dependent, proton-blocked AKT2/3 family. The homologous pore regions of AKT3 (amino acids 216 to 287) and KST1 (amino acids 217 to 289) have been exchanged to generate the two chimeric channels AKT3/(p)KST1 and KST1/(p)AKT3. In contrast to AKT3 wild-type channels, AKT3/(p)KST1 revealed a strong inward rectification reminiscent of that of KST1. Correspondingly, the substitution of the KST1 by the AKT3 pore led to less pronounced rectification properties of KST1/(p)AKT3 compared with wild-type KST1. Besides the voltage dependence, the interaction between the chimera and extracellular H^+ and Ca^{2+} resembled the properties of the inserted rather than the respective wild-type pore. Whereas AKT3/(p)KST1 was acid activated and Ca^{2+} insensitive, extracellular protons and Ca^{2+} inhibited KST1/(p)AKT3. The regulation of the chimeric channels by cytoplasmic protons followed the respective wild-type backbone of the chimeric channels, indicating that the intracellular pH sensor is located outside the P domain. We thus conclude that essential elements for external pH and Ca^{2+} regulation and for the rectification of voltage-dependent K^+ uptake channels are located within the channel pore.

INTRODUCTION

The function of the majority of K^+-transporting plant channel proteins depends on the membrane voltage. Among the isolated, functionally expressed, and electrophysiologically characterized K^+ channels, three different channel types can be distinguished with respect to their voltage-dependent gating: (1) outward-rectifying (KCO1, SKOR, and GORK) (Czempinski et al., 1997; Gaymard et al., 1998; Ache et al., 2000), (2) inward-rectifying (e.g., KAT1, AKT1, and KST1) (Anderson et al., 1992; Sentenac et al., 1992; Schachtman et al., 1994; Müller-Röber et al., 1995), and (3) weakly voltage-dependent K^+ channels (AKT2/3 and ZMK2) (Marten et al., 1999; Philippar et al., 1999; Lacombe et al., 2000). With the exception of KCO1 exhibiting four transmembrane helices and two pore regions, the voltage-dependent K^+ channels contain six putative transmembrane segments (S1 to S6) including an ion-conducting pore region P and a highly charged S4 segment (Doyle et al., 1998; Durell et al., 1998; Uozumi et al., 1998). The S4 domain of these plant K^+ channels is important for sensing changes in the membrane electric field (Dreyer et al., 1997; Hoth et al., 1997a; Marten and Hoshi, 1998). It does not, however, exclusively represent the voltage-sensing structure. Both the N and C termini affect the voltage-dependent gating behavior, too (Marten and Hoshi, 1997, 1998). Furthermore, single mutations in the P region of the guard cell inward rectifiers KAT1 and KST1 modulated the voltage dependence of the channel proteins, suggesting a role for the pore in the gating process (Becker et al., 1996; Hoth et al., 1997b). Regarding the distinct rectification properties, however, it is unclear why the six-transmembrane K^+ channels share not only the same overall structure but even the highly charged S4 segment.

Apart from the differences in the voltage-dependent gating, members of the KAT1 (KAT1 and KST1) and AKT2/3 (AKT3 and ZMK2) plant K^+ channel families differ in their regulation by extracellular protons and sensitivity toward extracellular calcium ions. Whereas KAT1 and KST1 are activated by external acidification due to a positive shift of the half-maximal activation voltage (Hedrich et al., 1995; Müller-Röber et al., 1995; Hoth et al., 1997b; Hoth and Hedrich, 1999a), AKT3 and ZMK2 are inhibited by an increased proton concentration (Marten et al., 1999; Philippar et al., 1999). This inhibition of AKT3 resulted from a decrease of the single-channel conductance, indicating an H^+ block of the K^+

[1] Both authors contributed equally to this study.

[2] Current address: Laboratory of Plant Molecular Biology, The Rockefeller University, 1230 York Avenue, New York, NY 10021-6399.

[3] To whom correspondence should be addressed. E-mail hedrich@botanik.uni-wuerzburg.de; fax 49-931-8886157.

channel pore (Marten et al., 1999; Lacombe et al., 2000). In KST1, essential molecular elements of the pH sensor could be identified using site-directed mutagenesis and electrophysiological analysis of the channel mutants (Hoth et al., 1997b; Hoth and Hedrich, 1999a). Whereas the simultaneous substitution of the only two extracellular histidine residues in KST1, located in the S3–S4 linker (H160) and in the channel pore (H271), generated a pH-insensitive mutant, the mutation of the pore histidine at position 271 into an arginine resulted in a channel mutant with an inverted pH regulation compared with the wild type (Hoth et al., 1997b). In contrast to KST1, the molecular structure of the pH sensor in AKT3 has not been characterized.

Patch-clamp studies on isolated protoplasts from different plant cells and species showed that extracellular Ca^{2+} ions block K^+ uptake channels in a voltage-dependent manner (Wegner et al., 1994; Roberts and Tester, 1995; Thiel et al., 1996; Dietrich et al., 1998). Whereas the susceptibility toward Ca^{2+} of the cloned guard cell α-subunits KAT1 and KST1 was very low (Brüggemann et al., 1998; Dreyer et al., 1998), AKT3 was significantly blocked by physiological concentrations of external Ca^{2+} (Marten et al., 1999). Although the voltage-dependent properties suggested that the Ca^{2+} ions partially enter the channel pore, the Ca^{2+} binding site remained unknown.

In this study, we generated chimeric channels between KST1 and AKT3 by exchanging the pore region of AKT3 (amino acids 216 to 287) and the homologous region of KST1 (amino acids 217 to 289). The electrophysiological characterization of these chimeric channels in Xenopus oocytes revealed that the channel pore plays a crucial role in the voltage-dependent gating of K^+ channels and harbors all basic molecular structures required for extracellular pH regulation and Ca^{2+} block.

RESULTS

To investigate the role of the pore region of plant K^+ uptake channels in rectification, Ca^{2+} inhibition, and pH regulation, we generated chimeric channels between KST1 and AKT3.

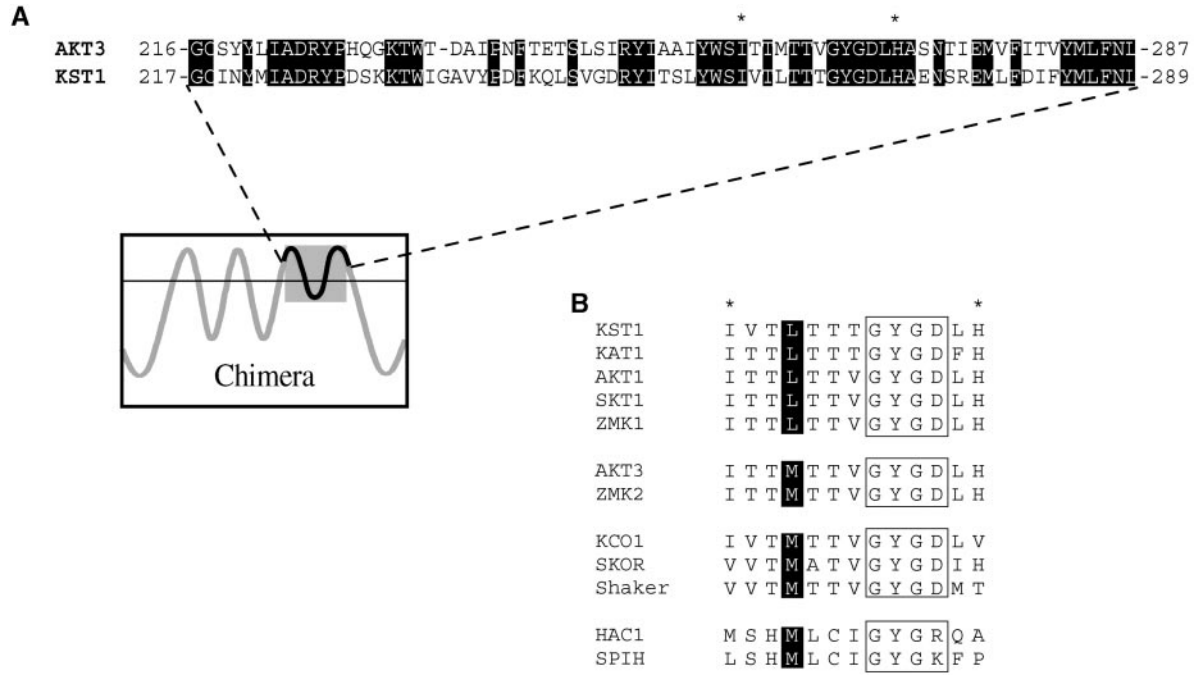

Figure 1. Alignments of Amino Acids within the Pore Region of K^+ Channels.

(A) Alignment of the pore region with parts of S5 and S6 of the voltage-dependent K^+ channels AKT3 and KST1. Amino acids 216 to 287 of AKT3 and amino acids 217 to 289 of KST1 are shown. The identical residues in both channel proteins are highlighted by black boxes. A schematic model of the membrane topology of the chimeric channels indicates the exchanged fragment.

(B) Alignment of plant and animal K^+ channel amino acid sequences in the pore region. Ten amino acids (c.f. sequence marked by asterisks in **[A]**) including the selectivity filter GYGD motif (boxed) are shown for the indicated K^+ channels. Four amino acids upstream, the GYG sequence conserved leucine and methionine residues are marked by black boxes. The GenBank accession numbers of the aligned channels sequences are as follows: KST1, X79779; KAT1, M86990; AKT1, X62907; SKT1, X86021; ZMK1; Y07632; AKT3, U44745; ZMK2, AJ132686; KCO1, X97323; SKOR, AJ223358; *Shaker*, M17211; HAC1, AJ225122; SPIH1, Y16880.

The channel pore of AKT3 with parts of S5 and S6 (amino acids 216 to 287) was substituted by the homologous region of KST1 (amino acids 217 to 289) and vice versa, as shown in Figure 1. In this particular region, both channels share ~58% identity on the amino acid level. The electrophysiological properties of the resulting chimeric channels AKT3/(p)KST1 and KST1/(p)AKT3 were studied in double-electrode voltage-clamp experiments after heterologous expression in Xenopus oocytes.

Voltage Dependence

Typical current recordings of AKT3 wild-type channels in the voltage range of +40 to −150 mV are shown in Figure 2A (left side). Both the instantaneous and the time-dependent current components were mediated by the AKT3 gene product (c.f. Marten et al., 1999). At voltages more positive than the K^+ equilibrium potential ($V_{rev} \approx 0$ mV), outward currents through AKT3 were elicited. The steady state currents (I_{ss}) plotted against the membrane voltage clearly visualize the weak voltage dependence and rectification of AKT3 (Figure 2B, left side). KST1, however, revealed a strong inward rectification conducting K^+ ions only upon hyperpolarization to voltages less than −90 mV (Figures 2A and 2B, second right). In contrast to AKT3 but in line with KST1, the chimera AKT3/(p)KST1 containing the KST1 pore exhibited the voltage-dependent properties of an inward rectifier lacking an AKT3-like instantaneous current component (Figures 2A and 2B, second left). Outward currents of oocytes expressing AKT3/(p)KST1 did not differ from background outward currents of KST1 (Figures 2A and 2B, second left) or noninjected oocytes (not shown; $n > 100$). KST1 lost its strong rectification after substitution of its native pore by the AKT3 pore (Figures 2A and 2B, right side). The chimera KST1/(p)AKT3 mediated K^+ efflux at membrane potentials positive of the K^+ equilibrium potential and resembled the two current components that are characteristic for AKT3. Instantaneous currents could be observed at positive and negative voltages, whereas the time-dependent current was restricted to voltages more negative than −90 mV (Figure 2A, right side). In >100 control experiments, outward currents of this magnitude and instantaneous current components have not been observed in either noninjected or KST-expressing oocytes.

A detailed analysis of the voltage dependence of the chimeric channels compared with the wild-type channels has been performed using Boltzman statistics. Figure 2C shows the open probabilities p_o plotted against the membrane voltage. The chimera AKT3/(p)KST1 ($V_{1/2} = -147 \pm 0.9$ mV, apparent gating charge $z = 1.65 \pm 0.03$) revealed voltage-dependent gating characteristics identical to KST1 ($V_{1/2} = -143 \pm 0.8$ mV, $z = 1.63 \pm 0.04$) but completely different from wild-type AKT3 ($V_{1/2} = -112 \pm 4.5$ mV, $z = 0.66 \pm 0.07$). This indicated that the KST1 pore was sufficient to confer a strong inward rectification on the channel. The substitution of the KST1 pore by the AKT3 pore in KST1/(p)AKT3 resulted in a decreased steepness of the p_o/V-curve ($V_{1/2} = -130 \pm 2.9$ mV, $z = 0.90 \pm 0.09$). This chimeric channel also resembled the AKT3-like minimal open probability different from zero at membrane voltages positive to −40 mV (c.f. Marten et al., 1999). However, its voltage-dependent gating parameters $V_{1/2}$ and z as well as the minimal open probability were slightly different from AKT3, indicating that other components of the AKT3 backbone might be needed for a complete conversion.

To identify residues in the P region that could account for the differences in rectification among members of the KAT1, AKT1, and AKT2/3 channel family, respectively, we compared the channels with respect to their amino acid sequences in the pore (Figure 1B). Whereas all members of the inward-rectifying KAT1 and AKT1 families contain a leucine residue four amino acids upstream of the GYGD sequence of the selectivity filter, a methionine is highly conserved at the identical position in the AKT2/3 family. This methionine residue is also present in outward-rectifying K^+ channels of the *Shaker* family as well as in the plant outward rectifiers SKOR and KCO1 (Figure 1B). To study the possible role of this residue for the rectification properties of K^+ channels, we generated the channel mutants AKT3-M260L and KST1-L262M. Like AKT3, the single mutant AKT3-M260L mediated K^+ influx and efflux, resembling the weak voltage dependence and the proton inhibition of the wild type (Figure 3, upper traces). The strong inward rectification and the acid activation of wild-type KST1 were unaffected in the mutant KST1-L262M (Figure 3B, lower traces). Thus, our analyses regarding the site-directed channel mutants KST1-L262M and AKT3-M260L identified that this position was not fundamental for the rectification of voltage-regulated K^+ channels. This finding is supported by Gauss et al. (1998) and Ludwig et al. (1998), showing that the animal six-transmembrane K^+ channels HAC1 and SPIH containing a methionine residue at the respective position represent, in fact, inward rectifiers (Figure 1B). Future experiments based on scanning mutagenesis are therefore required to identify structural determinants for rectification in the pore region of voltage-dependent K^+ channels.

Interaction with External Cations

Structural domains responsible for proton block and Ca^{2+} inhibition of AKT3 are most likely located in the pore of the channel protein. To obtain further information about the respective binding sites, we investigated the Ca^{2+} sensitivity and pH dependence of AKT3/(p)KST1 and KST1/(p)AKT3.

Calcium

Figure 4A shows the susceptibility of AKT3/(p)KST1 to extracellular Ca^{2+} in comparison to AKT3 wild-type channels.

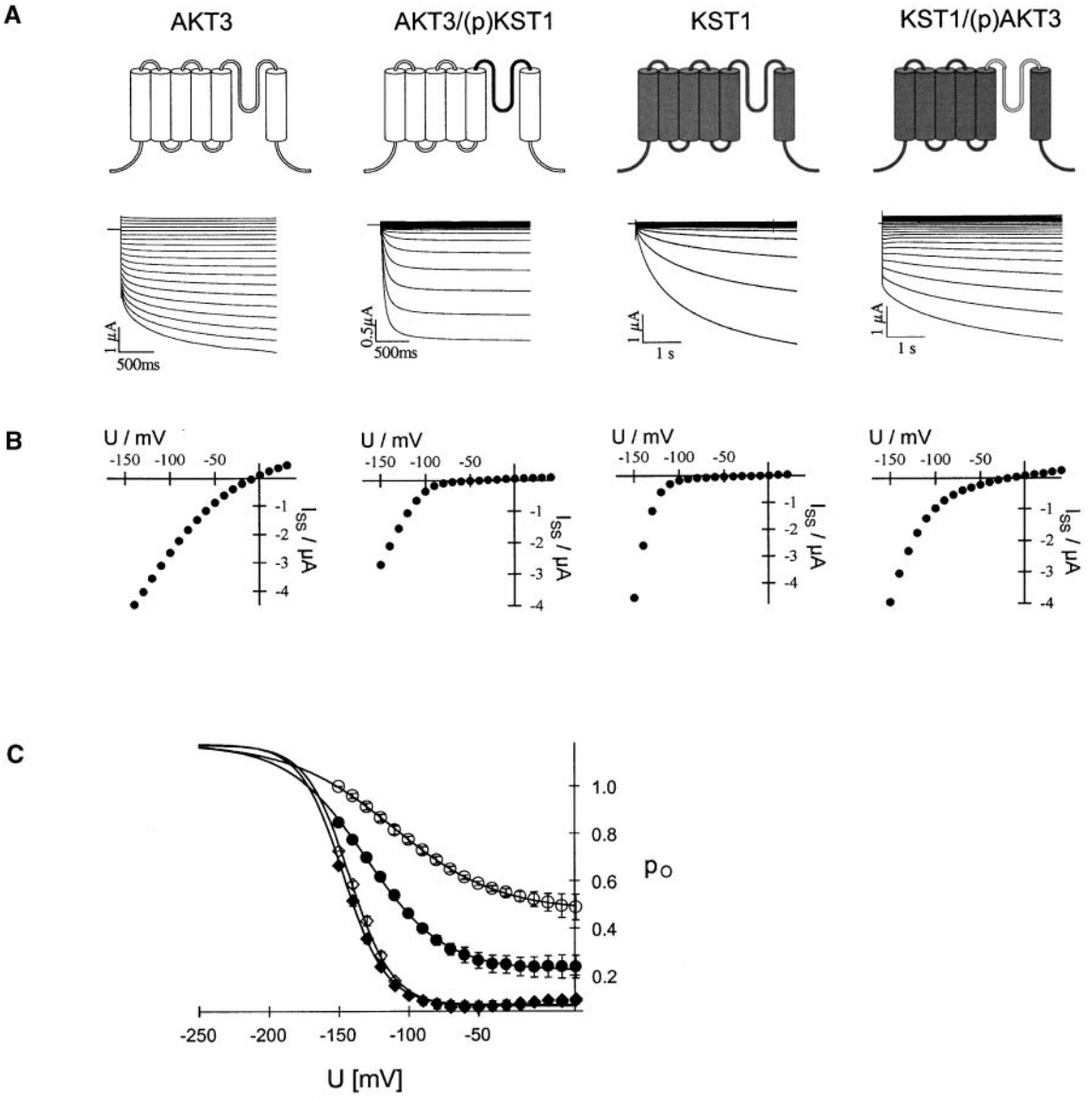

Figure 2. Voltage-Dependent Properties of AKT3, AKT3/(p)KST1, KST1, and KST1/(p)AKT3.

(A) Representative current traces in response to voltage pulses from +40 to −150 mV of AKT3 (left traces), KST1 (second right traces), and the chimeric channels AKT3/(p)KST1 (second left traces) as well as KST1/(p)AKT3 (right traces). Voltage pulses were applied in 10-mV decrements from a holding voltage of −10 mV for AKT3 and KST1/(p)AKT3 and −20 mV for KST1 and AKT3/(p)KST1, respectively. Oocytes with similar expression levels have been selected. AKT3 as well as KST1/(p)AKT currents were recorded at $pH_{ext.}$ 7.4, whereas KST1 and the chimera AKT3/(p)KST1 were recorded at $pH_{ext.}$ 5.6.

(B) The steady state currents I_{ss} were derived from the data shown in **(A)** and plotted against the membrane voltage. Note pronounced outward currents in AKT3 and KST1/(p)AKT3 but not in KST1 and AKT3/(p)KST1 in **(A)** and **(B)**.

(C) The open probabilities p_o in 30 mM K^+ and pH 7.4 for KST1 (◇), AKT3 (○), KST1/(p)AKT3 (●), and AKT3/(p)KST1 (◆) were plotted against the membrane voltage. Solid lines represent best Boltzman fits to the data. Error bars indicate standard deviation ($n = 3$).

In the presence of 20 mM K^+ and 30 mM Ca^{2+}, tail-current recordings in the range of +20 to −170 mV were performed after preactivating the channels at a membrane voltage of −150 mV. Whereas AKT3 resembled the characteristics of a voltage-dependent Ca^{2+} block (c.f. Marten et al., 1999), the chimera AKT3/(p)KST1 was Ca^{2+} insensitive even in the presence of 30 mM Ca^{2+}. The lack of a divalent cation block therefore corresponds with the Ca^{2+} phenotype observed for KST1 (Figure 4B; Brüggemann et al., 1998). Equipped with the AKT3 pore, however, KST1 became more sensitive to extracellular Ca^{2+}. Under identical experimental conditions, the chimera KST1/(p)AKT3 was blocked by Ca^{2+} at membrane voltages less than −110 mV in a voltage-dependent manner (Figure 4B).

Protons

The hyperpolarization-induced inward K^+ currents through AKT3/(p)KST1 reversibly increased upon a drop in the extracellular solution from pH 7.4 to 5.6 (Figure 4C). As shown for KST1 (Hoth et al., 1997b), the acid activation in this chimera was accompanied by a positive shift of the half-maximal activation voltage $V_{1/2}$ ($\Delta V_{1/2}$ = 13.1 ± 1.5 mV, n = 4). Thus, the replacement of the AKT3 by the KST1 pore in AKT3/(p)KST1 transformed the proton-blocked AKT3 into an acid-activated inward rectifier. Accordingly, the acid activation of KST1 was converted into an inhibition of K^+ influx by external protons in the chimera KST1/(p)AKT3, as demonstrated by a decrease in steady state currents of −77.9 ± 5.9% at −150 mV (Figure 4D).

Separation of the Intra- and Extracellular pH Sensor

Recently, Tang et al. (2000) showed that the intracellular pH sensor of the *Arabidopsis thaliana* guard cell K^+ uptake channel KAT1 is located in the cytosolic linker between the transmembrane helices S2 and S3. A histidine residue in this linker (H118) was fundamental for pH-sensitive changes in activation kinetics but not for the proton-induced shift in the half-maximal activation voltage. Because this domain was not substituted in the two chimeric channels, the dependence on internal protons should remain unaffected compared with AKT3 and KST1 wild-type channels, respectively. To confirm this prediction, 10 mM Na-acetate at pH 5.6 was applied to the extracellular solution. The nondissociated acid is able to permeate across the membrane and to release protons into the cell (c.f. Lacombe et al., 2000). Whereas KST1, like KAT1 (Tang et al., 2000), was activated by increasing the intracellular proton concentration (29.4 ± 2.9% at −130 mV; Figure 5C), AKT3 was inhibited by cytosolic acidification (−66.5 ± 6.3% at −130 mV; Figure 5A). Like AKT3 in the presence of 10 mM acetate, the currents through AKT3/(p)KST1 were almost completely suppressed (−59.2 ± 7.0% at −130 mV; Figure 5B). Although KST1/(p)AKT3-mediated currents are largely inhibited at pH 5.6 in the bath (c.f. Figure 4D), the equipment of KST1 with the AKT3 pore did not affect the cytosolic pH regulation of KST1. As for the wild type (Figure 5C), the acidification of the cytoplasm resulted in an increased inward current (62.4 ± 2.7% at −130 mV; Figure 5D). These results therefore provide strong evidence that the pore region of K^+ uptake channels does not interact with intracellular protons. As a

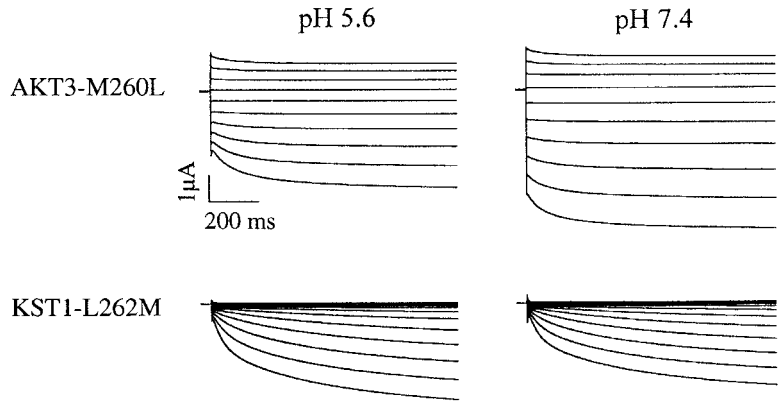

Figure 3. Voltage and pH Regulation of AKT3-M260L and KST1-L262M.

K^+ currents in 30 mM K^+ of the channel mutants AKT3-M260L (upper traces) and KST1-L262M (lower traces) were recorded at membrane voltages in the range from +30 to −150 mV. From the holding voltage of −33 mV and −20 mV for AKT3-M260L and KST1-L262M, respectively, the membrane voltage was changed in steps of −20 mV. Upon a change in the extracellular pH from 5.6 to 7.4, K^+ currents through AKT3-M260L increased (42.8 ± 1.2% at −130 mV), whereas those through KST1-L262M decreased (−27.6 ± 6.4% at −130 mV). For both channel mutants, representative current recordings out of three to four experiments are shown. The observed changes in steady state currents during the pH shift experiments were significantly different in the voltage range from −80 to −150 mV ($P < 0.01$).

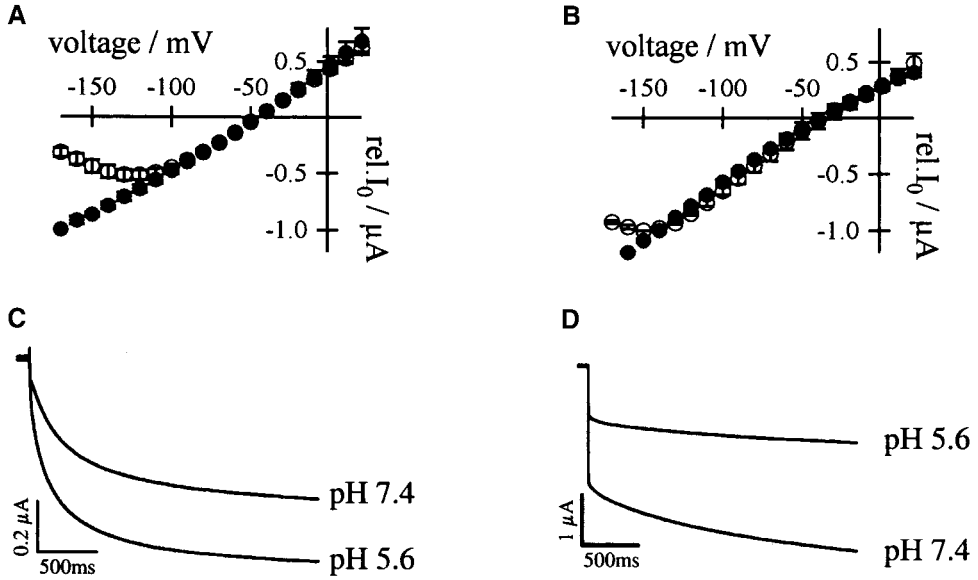

Figure 4. Dependence of AKT3/(p)KST1 and KST1/(p)AKT3 on Extracellular Ca^{2+} and H^+.

(A) Relative (rel.) instantaneous tail-current amplitudes I_0 plotted against the membrane voltage revealed a voltage-dependent Ca^{2+} block for AKT3 (○, $n = 3$) but not for the chimeric channels AKT3/(p)KST1 (●, $n = 3$). The Ca^{2+} solution contained 20 mM KCl, 10 mM Tris/Mes, pH 7.2, and 30 mM $CaCl_2$. In the control solution, $CaCl_2$ was replaced with 30 mM $MgCl_2$. Error bars were smaller than symbols and represent the standard deviation ($n \geq 3$). I_0 currents in the presence of calcium were significantly different in the voltage range of −130 to −170 mV for the chimera AKT3/(p)KST1 compared with AKT3 wild type ($P < 0.01$).

(B) Superimposed I_0/V-plot of KST1 and KST1/(p)AKT3 . Under the same experimental conditions as described in **(A)**, the chimera KST1/(p)AKT3 was blocked by extracellular Ca^{2+} (○, $n = 4$) in contrast to KST1 wild type (●, $n = 3$). Error bars were smaller than symbols and represent the standard deviation ($n \geq 3$). I_0 currents in the presence of calcium were significantly different in the voltage range of −150 to −170 mV for the chimera KST1/(p)AKT3 compared with KST1 wild type ($P < 0.01$).

(C) Acid-activated inward K^+ currents of AKT3/(p)KST1 in response to 2.5-sec voltage pulses to −150 mV from the holding voltage of −20 mV. Currents were recorded in the presence of standard external media buffered to pH values as indicated.

(D) Voltage pulses to −150 mV from the holding voltage of −20 mV elucidated that K^+ currents of KST1/(p)AKT3 decreased upon a change from pH 7.4 to 5.6.

(C) and **(D)** show representative current traces out of four independent experiments. Steady state currents in **(C)** and **(D)** at pH 5.6 were significantly different from currents at pH 7.4 at −150 mV ($P < 0.01$).

consequence, it is very unlikely that extracellular protons reach the internal pH sensor via the pore.

DISCUSSION

The generation of point mutations and chimeric channels led to the identification of the S4 segment as well as the N and C termini as important elements of the voltage-sensing structure of *Shaker*-like K^+ channels (Papazian et al., 1991; Perozo et al., 1994; Tytgat et al., 1994; Yusaf et al., 1996; Dreyer et al., 1997; Hoth et al., 1997a; Marten and Hoshi, 1997; Terlau et al., 1997; Chanda et al., 1999; Chiara et al., 1999). Here, we show that the pore region contributes to the rectification of voltage-dependent plant K^+ channels. On one hand, the substitution of the pore region including parts of S5 and S6 in the chimeric channel AKT3/(p)KST1 was sufficient to transform the weak voltage-dependent AKT3 into an inward rectifier (Figures 2A and 2B, left). On the other hand, KST1 equipped with the AKT3 pore lost its strong inward rectification (Figures 2A and 2B, right). In KAT1 and KST1, several point mutations in the P region resulted in a modulation of the voltage-dependent gating (Becker et al., 1996; Hoth et al., 1997b). A molecular link between the pore and the putative voltage sensor S4 was therefore anticipated (Hoth and Hedrich, 1999a). The pore histidine (H271) and the histidine in the S3–S4 linker (H160), which represent key amino acids of the pH sensor of KST1, as well as the arginine at position 181 in the S4 segment have been proposed as putative elements within this molecular link. Furthermore, Zn^{2+} binding studies on KST1 wild type and histidine mutants suggested that the S3–S4 linker is involved in the formation of the outer mouth of the pore (Hoth and Hedrich, 1999b). Together with specific pore amino acids, this S3–S4 loop could link the movement of S4 to chan-

nel opening. This model would also explain the data obtained with chimeric channels between KAT1 and Xsha2 that located components for inward rectification in the first third of the KAT1 channel including S1 to S4 and the S4–S5 linker (Cao et al., 1995). Local protein arrangements in the pore underlying the slow inactivation of the *Shaker* channel have also been postulated from voltage clamp fluorometry experiments (Loots and Isacoff, 1998).

The difference in the Ca^{2+} sensitivity of voltage-dependent K^+ channels results from distinct amino acids in the channel pore. Upon replacement of the AKT3 pore by the KST1 pore, which is almost Ca^{2+} insensitive (Brüggemann et al., 1998), AKT3/(p)KST1 lost its Ca^{2+} susceptibility (Figure 4A). The AKT3 pore, however, transformed the Ca^{2+} phenotype of KST1 from weakly sensitive to Ca^{2+} blocked (Figure 4B). Our experiments concerning the dependence of the chimeric channels on extracellular protons show that the pore of KST1 is sufficient to confer the acid activation of AKT3/(p)KST1 (Figure 4C). As deduced from a proton-induced decrease of the single-channel conductance (Marten et al., 1999), the binding site for protons seems to be located in the AKT3 pore. This was confirmed by the proton inhibition of KST1/(p)AKT3 (Figure 4D). Because the mutant AKT3-M262L is still inhibited by protons (Figure 3), this residue reminiscent of members of the AKT2/3 channel family does not account for the proton block of AKT3. The comparison of residues within the exchanged 60–amino acid pore peptide between AKT3 and KST1, however, limits the putative candidates for the binding site to 29 amino acids. Future analysis of the conserved exchanges between both channels and site-directed mutations should therefore identify the key amino acids of the Ca^{2+} binding site as well as the pH sensor of AKT3.

On the basis of studies with the chimera, we were able to

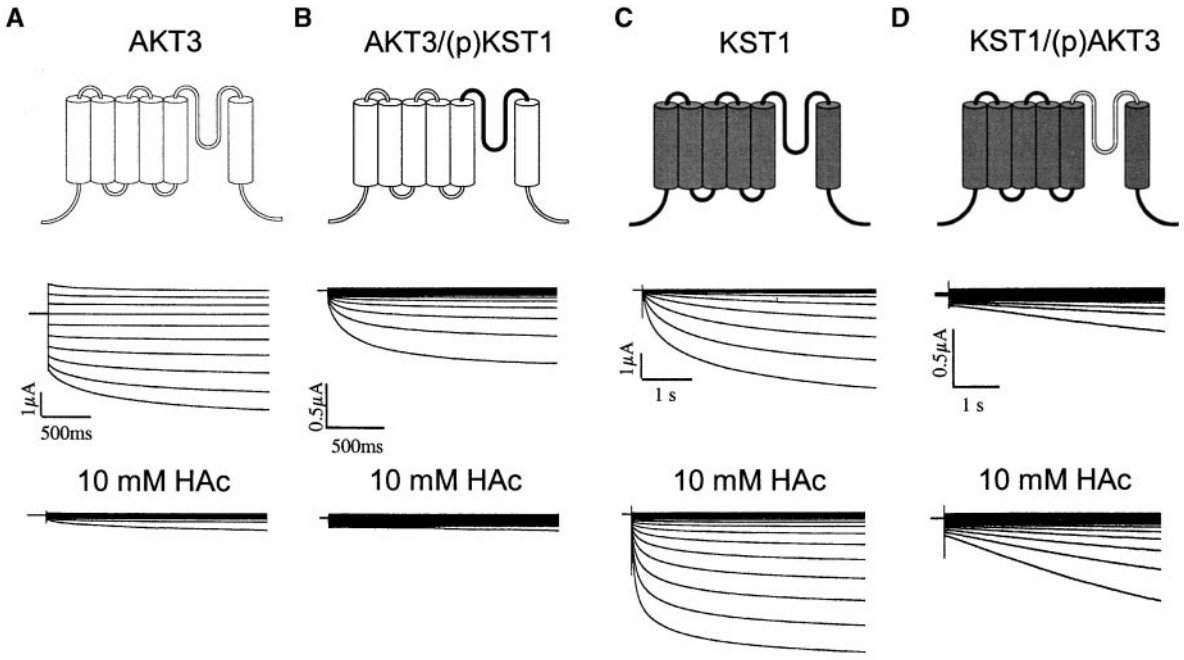

Figure 5. Regulation of AKT3, AKT3/(p)KST1, KST1, and KST1/(p)AKT3 by Intracellular Protons.

(A) In the voltage range of +30 to −150 mV, voltage pulses from a holding voltage of −30 mV in steps of 20 mV for a duration of 2.5 sec demonstrate the inhibition of K^+ fluxes through AKT3 in the presence of 10 mM acetate compared with control conditions ($n = 4$). Note the decrease of outward as well as inward K^+ currents.

(B) K^+ currents mediated by AKT3/(p)KST1 before and after addition of 10 mM acetate to the extracellular solution ($n = 3$). From the holding voltage of −20 mV, the membrane voltage was changed to −120 mV in 10-mV decrements.

(C) K^+ currents through KST1 were elicited by 5-sec voltage pulses in the range of +20 to −150 mV (10-mV decrements) in the absence and in the presence of 10 mM acetate ($n = 6$).

(D) Activation of K^+ inward currents through KST1/(p)AKT3 upon addition of 10 mM HAc. Current traces in response to voltages in the range from +30 to −130 mV (10-mV decrements) are shown ($n = 3$).

The solutions used for results shown in **(A)** to **(D)** were composed of 30 mM KCl, 1 mM $CaCl_2$, 2 mM $MgCl_2$, and 10 mM Mes/Tris, pH 5.6, as well as 10 mM NaCl or 10 mM Na-acetate, respectively. Steady state currents in the presence of sodium acetate were significantly different from those in sodium chloride in the voltage range from −80 to −130 mV ($P < 0.05$).

show that the intracellular pH sensor of voltage-dependent K^+ channels is distinct from the extracellular pH-sensing structure. This observation is supported by the following results. (1) AKT3 is inhibited by both external and internal protons, whereas the substitution of the pore provides the chimera AKT3/(p)KST1 with an activation upon extracellular acidification (Figure 4), leaving its intracellular pH dependence unaffected (Figure 5). (2) KST1 containing the AKT3 pore maintained its activation by intracellular protons (Figure 5). (3) The KST1 double mutant H160A/H271A, which is insensitive to external protons, still activated upon a pH drop in the cytoplasm (S. Hoth and R. Hedrich, unpublished results). In this context, it should be mentioned that the participation of the cytosolic S2–S3 linker in KAT1 in sensing intracellular pH changes has recently been shown (Tang et al., 2000).

In conclusion, the pore region of voltage-gated K^+ channels contains essential sites for H^+ and Ca^{2+} binding as well as for rectification. Future experiments on additional channel mutants and chimeric channels will help to identify the individual molecular entities of these fundamental processes.

METHODS

Generation of Chimeric Channels

For the generation of the chimeric channels, two site-directed silent mutations (QuikChange site-directed mutagenesis kit; Stratagene, Heidelberg, Germany) in AKT3 and KST1, respectively, were performed, introducing a BstXI and an AatI restriction site in both plasmids (pKST1#8 in the pGEMHE vector and pAKT3 in the pGEMA vector) at identical sites. In pAKT3, the BstXI site at position 644 was generated by primers 5′-TTGTTTCTAGTCCACTGTGCTGGATGCAG-3′ and 5′-CTGCATCCAGCACAGTGGACTAGAAACAA-3′ and the AatI site at position 864 was generated by primers 5′-GTTATTCAATCTAGGCCTCACTGCTTACC-3′ and 5′-GGTAAGCAGTGAGGCCTAGATTGAATAAC-3′. The primers 5′-TGTTTGCAGTCCACTGTGCTGGATGCATTAAC-3′ and 5′-GTTAATGCATCCAGCACAGTGGACTGCAAACA-3′ as well as primers 5′-TGTTATTCAACTTAGGCCTGACATCTTAC-3′ and 5′-GTAAGATGTCAGGCCTAAGTTGAATAACA-3′ were used to introduce the BstXI site at position 647 and the AatI site at position 870 in pKST1#8, respectively. Chimeric channels AKT3/(p)KST1 and KST1/(p)AKT3 were derived by exchanging the corresponding DNA fragments of pAKT3 and pKST1#8 between the generated BstXI and AatI sites. The cDNA sequences were verified by DNA sequence analysis (Thermo sequenase fluorescent labeled primer cycle sequencing kit with 7-deaza-dGTP; Amersham Pharmacia, Braunschweig, Germany). The single mutants AKT3-M260L and KST1-L262M were generated as described by Hoth and Hedrich (1999a).

Electrophysiology

The cRNAs of wild-type channels KST1 and AKT3 as well as the chimera were generated by in vitro transcription (T7-Megascript kit; Ambion Inc., Austin, TX) and injected into oocytes of *Xenopus laevis* (Nasco, Fort Atkinson, WI) using a Picospritzer II microinjector (General Valve, Fairfield, NJ). Two to 6 days after injection, double-electrode voltage-clamp recordings were performed with a Turbotec-01C amplifier (npi Instruments, Tamm, Germany). The electrodes were filled with 3 M KCl and had typical input resistances of 2 to 6 MΩ. Solutions were composed of 100 mM KCl, 2 mM $MgCl_2$, 1 mM $CaCl_2$, and 10 mM Tris/Mes or Mes/Tris, pH 7.4 and 5.6, respectively. For measurements with respect to changes in external Ca^{2+} and in the intracellular pH, the composition of solutions is listed in the legends to Figures 4 and 5. All media were adjusted to a final osmolality of 215 to 235 mosmol kg^{-1} with D-sorbitol. Analyses of voltage dependence, pH dependence, and Ca^{2+} block were performed as described previously (Hoth et al., 1997b; Marten et al., 1999). Data points with error bars represent the mean ±SD, and statistical significance was verified by a paired Student's *t* test.

ACKNOWLEDGMENTS

We are grateful to Petra Dietrich and Natalya Ivashikina for helpful comments on the manuscript. This work was supported by grants to R.H. from the Deutsche Forschungsgemeinschaft.

Received October 12, 2000; accepted January 29, 2001.

REFERENCES

Ache, P., Becker, D., Ivashikina, N., Dietrich, P., Roelfsema, R.M.G., and Hedrich, R. (2000). GORK, a delayed outward rectifier expressed in guard cells of *Arabidopsis thaliana*, is a K^+-selective, K^+-sensing ion channel. FEBS Lett. **486,** 93–98.

Anderson, J.A., Huprikar, S.S., Kochian, L.V., Lucas, W.J., and Gaber, R.F. (1992). Functional expression of a probable *Arabidopsis thaliana* potassium channel in *Saccharomyces cerevisiae*. Proc. Natl. Acad. Sci. USA **89,** 3736–3740.

Becker, D., Dreyer, I., Hoth, S., Reid, J.D., Busch, H., Lehnen, M., Palme, K., and Hedrich, R. (1996). Changes in the voltage activation, Cs^+ sensitivity, and ion permeability in H5 mutants of the plant K^+ channel KAT1. Proc. Natl. Acad. Sci. USA **93,** 8123–8128.

Brüggemann, L., Dietrich, P., Dreyer, I., and Hedrich, R. (1998). Pronounced differences between guard cell K^+ channels in vivo and their respective α-subunit homomers in *Xenopus* oocytes. Planta **207,** 370–376.

Cao, Y., Crawford, N.M., and Schroeder, J.I. (1995). Amino terminus and the first four membrane-spanning segments of the Arabidopsis K^+ channel KAT1 confer inward-rectification property of plant–animal chimeric channels. J. Biol. Chem. **270,** 17697–17701.

Chanda, B., Tiwari, J.K., Varshney, A., and Mathew, M.K. (1999). Transplanting the N-terminus from Kv1.4 to Kv1.1 generates an inwardly rectifying K^+ channel. Neuroreport **10,** 237–241.

Chiara, M.D., Monje, F., Castellano, A., and Lopez-Barneo, J. (1999). A small domain in the N terminus of the regulatory alpha-

subunit kv2.3 modulates kv2.1 potassium channel gating. J. Neurosci. **19,** 6865–6873.

Czempinski, K., Zimmermann, S., Erhardt, T., and Müller-Röber, B. (1997). New structure and function in plant K^+ channels: KCO1, an outward rectifier with a steep Ca^{2+} dependency. EMBO J. **16,** 3455–3463.

Dietrich, P., Dreyer, I., Wiesner, P., and Hedrich, R. (1998). Cation sensitivity and kinetics of guard-cell potassium channels differ among species. Planta **205,** 277–287.

Doyle, D.A., Cabral, J.M., Pfuetzner, R.A., Kuo, A., Gulbis, J.M., Cohen, S.L., Chait, B.T., and MacKinnon, R. (1998). The structure of the potassium channel: Molecular basis of K^+ conduction and selectivity. Science **280,** 69–77.

Dreyer, I., Antunes, S., Hoshi, T., Müller-Röber, B., Palme, K., Pongs, O., Reintanz, B., and Hedrich, R. (1997). Plant K^+ channel α-subunits assemble indiscriminately. Biophys. J. **72,** 2143–2150.

Dreyer, I., Becker, D., Bregante, M., Gambale, F., Lehnen, M., Palme, K., and Hedrich, R. (1998). Single mutations strongly alter the K^+-selective pore of the K_{in} channel KAT1. FEBS Lett. **430,** 370–376.

Durell, S.R., Hao, Y.H., and Guy, H.R. (1998). Structural models of the transmembrane region of voltage-gated and other K^+ channels in open, closed, and inactivated conformations. J. Struct. Biol. **121,** 263–284.

Gauss, R., Seifert, R., and Kaupp, B. (1998). Molecular identification of a hyperpolarization-activated channel in sea urchin sperm. Nature **393,** 583–587.

Gaymard, F., Pilot, G., Lacombe, B., Bouchez, D., Bruneau, D., Boucherez, J., Michaux-Ferriere, N., Thibaud, J.B., and Sentenac, H. (1998). Identification and disruption of a plant *Shaker*-like outward channel involved in K^+ release into the xylem sap. Cell **94,** 647–655.

Hedrich, R., Moran, O., Conti, F., Busch, H., Becker, D., Gambale, F., Dreyer, I., Küch, A., Neuwinger, K., and Palme, K. (1995). Inward rectifier potassium channels in plants differ from their animal counterparts in response to voltage and channel modulators. Eur. Biophys. J. **66,** 1061–1067.

Hoth, S., and Hedrich, R. (1999a). Distinct molecular bases for pH sensitivity of the guard cell K^+ channels KST1 and KAT1. J. Biol. Chem. **274,** 11599–11603.

Hoth, S., and Hedrich, R. (1999b). Susceptibility of the guard cell K^+ uptake channel KST1 towards Zn^{2+} requires histidine residues in the S3–S4 linker and in the channel pore. Planta **209,** 543–546.

Hoth, S., Dreyer, I., and Hedrich, R. (1997a). Mutational analysis of functional domains within plant K^+ uptake channels. J. Exp. Bot. **48,** 415–420.

Hoth, S., Dreyer, I., Dietrich, P., Becker, D., Müller-Röber, B., and Hedrich, R. (1997b). Molecular basis of plant-specific acid activation of K^+ uptake channels. Proc. Natl. Acad. Sci. USA **94,** 4806–4810.

Lacombe, B., Pilot, G., Michard, E., Gaymard, F., Sentenac, H., and Thibaud, J.-B. (2000). A *Shaker*-like K^+ channel with weak rectification is expressed in both source and sink phloem tissues of *Arabidopsis*. Plant Cell **12,** 837–851.

Loots, E., and Isacoff, E.Y. (1998). Protein rearrangements underlying slow inactivation of the *Shaker* K^+ channel. J. Gen. Physiol. **112,** 377–389.

Ludwig, A., Zong, X., Jeglitsch, M., Hofmann, F., and Biel, M. (1998). A family of hyperpolarization-activated mammalian cation channels. Nature **393,** 587–591.

Marten, I., and Hoshi, T. (1997). Voltage-dependent gating characteristics of the K^+ channel KAT1 depend on the N and C termini. Proc. Natl. Acad. Sci. USA **94,** 3448–3453.

Marten, I., and Hoshi, T. (1998). The N-terminus of the K channel KAT1 controls its voltage-dependent gating by altering the membrane electric field. Biophys. J. **74,** 2953–2962.

Marten, I., Hoth, S., Deeken, R., Ache, P., Ketchum, K.A., Hoshi, T., and Hedrich, R. (1999). AKT3, a phloem-localized K^+ channel, is blocked by protons. Proc. Natl. Acad. Sci. USA **96,** 7581–7586.

Müller-Röber, B., Busch, H., Ellenberg, J., Becker, D., Provart, N., Dietrich, P., Willmitzer, L., Hoth, S., and Hedrich, R. (1995). Cloning and electrophysiological analysis of KST1, an inward-rectifying K^+ channel expressed in potato guard cells. EMBO J. **14,** 2409–2416.

Papazian, D.M., Timpe, L.C., Jan, Y.N., and Jan, L.Y. (1991). Alteration of voltage-dependence of Shaker potassium channel by mutations in the S4 sequence. Nature **349,** 305–310.

Perozo, E., Santa-Cruz-Toloza, L., Stefani, E., Bezanilla, F., and Papazian, D.M. (1994). S4 mutations alter gating currents of *Shaker* K channels. Biophys. J. **66,** 345–354.

Philippar, K., Fuchs, I., Lüthen, H., Hoth, S., Bauer, C., Haga, K., Thiel, G., Ljung, K., Sandberg, G., Böttger, M., Becker, D., and Hedrich, R. (1999). Auxin-induced K^+ channel expression represents an essential step in coleoptile growth and gravitropism. Proc. Natl. Acad. Sci. USA **96,** 12186–12191.

Roberts, S.K., and Tester, M. (1995). Inward and outward K^+-selective currents in the plasma membrane of protoplasts from maize root cortex and stele. Plant J. **8,** 811–825.

Schachtman, D.P., Schroeder, J.I., Lucas, W.J., Anderson, J.A., and Gaber, R.F. (1994). Expression of an inward-rectifying potassium channel by the Arabidopsis KAT1 cDNA. Science **258,** 1654–1658.

Sentenac, H., Bonneaud, N., Minet, M., Lacroute, F., Salmon, J.M., Gaymard, F., and Grignon, C. (1992). Cloning and expression in yeast of a plant potassium ion transport system. Science **256,** 663–665.

Tang, X.D., Marten, I., Dietrich, P., Ivashikina, N., Hedrich, R., and Hoshi, T. (2000). Histidine^{118} in the S2–S3 linker specifically controls activation of the KAT1 channel expressed in *Xenopus* oocytes. Biophys. J. **78,** 1255–1269.

Terlau, H., Heinemann, S.H., Stühmer, W., Pongs, O., and Ludwig, J. (1997). Amino terminal–dependent gating of the potassium channel rat eag is compensated by a mutation in the S4 segment. J. Physiol. Lond. **502,** 537–543.

Thiel, G., Brüdern, A., and Gradmann, D. (1996). Small inward rectifying K^+ channels in coleoptiles: Inhibition by external Ca^{2+} and function in cell elongation. J. Membr. Biol. **149,** 9–26.

Tytgat, J., Vereecke, J., and Carmeliet, E. (1994). Reversal of rectification and alteration of selectivity and pharmacology in a mammalian Kv1.1 potassium channel by deletion of domains S1 to S4. J. Physiol. **481.1,** 7–13.

Uozumi, N., Nakamura, T., Schroeder, J.I., and Muto, S. (1998). Determination of transmembrane topology of an inward-rectifying potassium channel from *Arabidopsis thaliana* based on functional expression in *Escherichia coli*. Proc. Natl. Acad. Sci. USA **95,** 9773–9778.

Wegner, L.H., De Boer, A.H., and Raschke, K. (1994). Properties of the K^+ inward rectifier in the plasma membrane of xylem parenchyma cells from barley roots: Effects of TEA^+, Ca^{2+}, Ba^{2+} and La^{3+}. J. Membr. Biol. **142,** 363–379.

Yusaf, S.P., Wray, D., and Sivaprasadarao, A. (1996). Measurement of the movement of the S4-segment during the activation of a voltage-gated potassium channel. Pflügers Arch. **433,** 91–97.